CALCIUM CONTENT OF WHEAT KERNEL SECTIONS BY CRITICAL MICRORADIOGRAPHY[1]

R. KATZ AND M. R. QUERRY

ABSTRACT

Calcium segregations in thin sections of wheat endosperm were mapped by means of radiographs made with monochromatic X-rays whose wave lengths were on either side of the K critical absorption edge of calcium. Concentrations of calcium were observed within endosperm cell walls in some kernels, and generalized nonuniform distribution of calcium was observed in others.

Earlier investigators (1,2) have shown mineral heterogeneity within macroscopic regions of wheat endosperm when material was extracted from a kernel with a dental burr. Our investigation sought to map calcium content in greater detail. This was done by using pairs of radiographs made of thin sections of wheat endosperm which were critically sensitive to calcium. The calcium content of a volume of endosperm as small as 0.018 mm.^{3} was determined. The techniques clearly are not restricted to calcium. Their applicability to other minerals is being investigated.

Materials and Methods

The Absorption of X-Rays. The decrease in intensity of a collimated monochromatic X-ray beam which passes through a monoelemental absorber is given by the equation

$$I = I_0 e^{-\mu m}, \qquad (1)$$

where I_0 is the intensity of the incident beam, I is the intensity of the emergent beam, μ is the mass absorption coefficient of the absorber element, and m is the mass per unit area of the absorbing material in the path of the beam (3, p. 172). In the wave-length region of interest

[1]Manuscript received August 3, 1964. Contribution No. 98, Department of Physics, Kansas Agricultural Experiment Station, Manhattan.

here, the intensity decrease is due to two processes: The first is the scattering of incident radiation from the collimated beam; the second, and of central importance to this investigation, is the photoelectric absorption of incident X-rays by the bound electrons of the absorber atoms.

At short wave lengths, X-radiation is most penetrating and the absorption coefficient is low. As the wave length increases, the mass absorption coefficient increases according to the relation

$$\mu = k\ \lambda^n, \qquad (2)$$

where k is a proportionality constant, and n is close to 3. The absorption coefficient decreases markedly (3, p. 318) when a critical wave length λ_K, characteristic of the absorber element and known as the K critical absorption edge, is reached. X-rays of wave length greater than λ_K have insufficient energy to remove electrons from the K shell of the absorber atoms, so that the photoelectric contribution of these electrons to the mass absorption coefficient is abruptly eliminated. From λ_K the mass absorption coefficient again increases, following equation 2 but with different values of k and n. Curve A of Fig. 1 is a log-log plot of the mass absorption coefficient *vs.* wave length for calcium absorbers. Chemical combination, which involves outer shell electrons, does not influence the absorption coefficient in any significant way. The fact that X-ray absorption in the vicinity of a

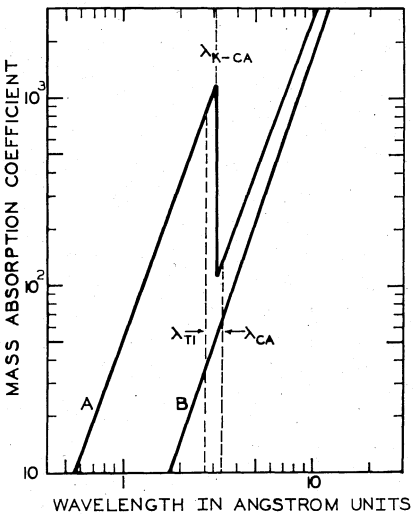

Fig. 1. Curve A is a log-log plot of mass absorption coefficient compared with wave length for the element calcium. Curve B shows the mass absorption coefficient of plant protein, assuming it to consist of 6% H, 54% C, 17% N, and 23% O. $\lambda_{Ti} = 2.750$A, $\lambda_{K-Ca} = 3.070$A, $\lambda_{Ca} = 3.360$A.

K edge depends on the atomic concentration and not on the state of chemical combination (4, p. 7) enables us to determine the mass per unit area of the critical absorber element, in the absorbing sample.

Wheat consists primarily of hydrogen, carbon, nitrogen, and oxygen (HCNO), whose mass absorption coefficient is generally less than that of calcium. Curve B of Fig. 1 shows the mass absorption coefficient of plant protein computed from the elemental composition and elemental absorption coefficient, and it is most important that the absorption of X-rays in plant protein varies smoothly with wave length in the region of the K absorption edge of calcium. A similar curve could be drawn for plant carbohydrate.

The Fluorescent X-Ray Camera. From the preceding discussion it is clear that the determination of calcium content by X-ray absorption depends on noting differences in absorption in a particular specimen when well-defined wave lengths on either side of the absorption edge are used.

Nearly monochromatic X-rays characteristic of the target material can be obtained from replaceable target X-ray tubes by filtering out the background continuous spectrum. This technique seriously limits the number of monochromatic X-ray beams that can be obtained, since the physical properties of many elements forbid their use as X-ray tube targets. These same elements can be used external to an X-ray tube as a source of fluorescent X-rays, for, when a chemical element is irradiated with a carefully chosen polychromatic X-ray beam, the photoelectric absorption of the primary beam leaves vacancies in the inner shells of the absorbing element. Outer electrons fall into the vacancies in the inner shells, producing secondary fluorescent X-rays characteristic of the element irradiated.

Other investigators (5,6,7) have shown that highly monochromatic fluorescent beams, whose intensity is sufficient for the radiography of thin specimens, can be obtained by use of an X-ray tube with a thin beryllium window as the source of the primary radiation. Fluorescent cameras have been constructed and have been applied to problems in metallurgy and biology.

The fluorescent X-ray camera constructed for this work is shown in Fig. 2. A threaded brass plug *A* attaches to the anode shield of a Machlett AEG-50 tungsten target, beryllium-window X-ray tube which is powered by a Picker 50-kv. industrial X-ray unit; *B* is a lead-lined port which partially collimates the primary beam used to irradiate the secondary target *C*. Fluorescent radiation from the target *C* passes through a helium atmosphere, contained in chamber *D*, which is pro-

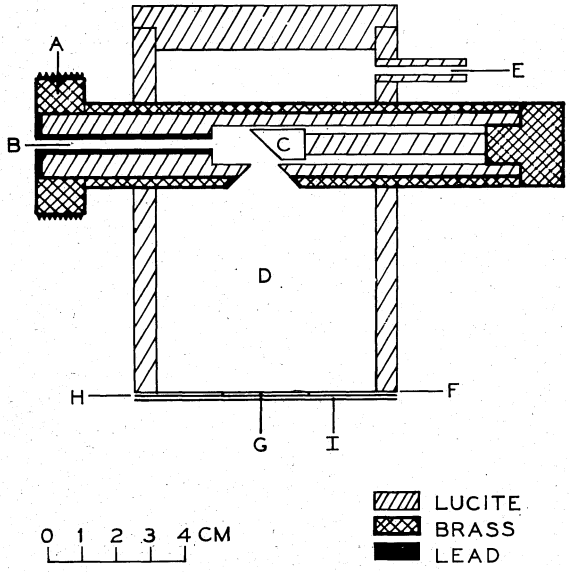

Fig. 2. Fluorescent X-ray camera.

vided with an inlet port *E*, and through a 0.00025-in. Mylar diaphragm *F*, which is backed by a thin polyethylene disk *I*. The positive helium pressure serves to hold the specimen *G* between the Mylar diaphragm and the polyethylene disk, in intimate contact with the X-ray film *H*. The camera design was evolved in response to the need to minimize scattered primary radiation. A helium path is used because the soft fluorescent X-rays are readily absorbed in air.

The monochromaticity of the fluorescent beams was checked by plotting aluminum absorption curves for the fluorescent radiation from a cobalt secondary target, as shown in Fig. 3. Here the experimental absorption curve was obtained by use of an aluminum-foil step block, and photographic film detection exposed in its linear response range (see Appendix I). The relative intensity was plotted against the thickness of aluminum and was decomposed into two straight lines. One line, A, represents the fluorescent radiation and the other line, B, represents the scattered radiation from the secondary target. The absorption coefficient obtained for the fluorescent component was 63.5 cm.^{2} per g., in reasonable agreement with the tabular value of 73 cm.^{2} per g. for the absorption of radiation of this wave length in aluminum. The point at which line *B* intersects the ordinate, 0.1, represents the relative intensity of the radiation scattered from the secondary target. The absorption coefficient represented by

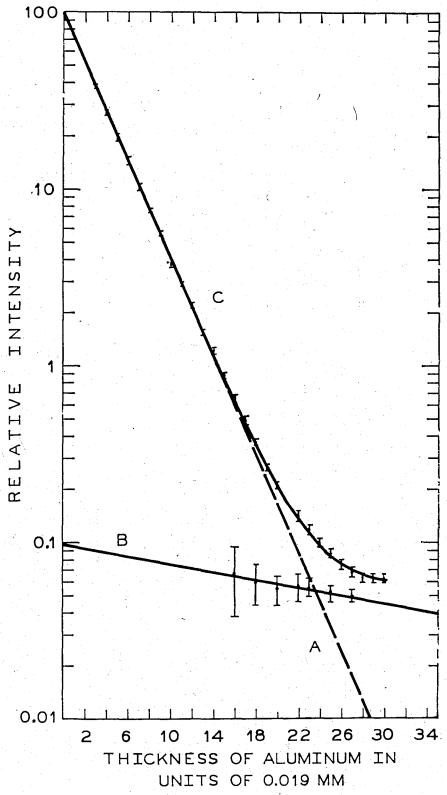

Fig. 3. Curve C is a semilog plot of an experimental aluminum absorption curve for fluorescent Cobalt K_α radiation. Curve A represents the fluorescent radiation, and curve B, scattered radiation. Exposures were at 20.3 peak kilovolts (pkv.) and 20 ma.

this curve was 5 cm.^{2}/g., which is consistent with a wave length of 0.7A, within the continuous spectrum of the primary beam. In this experiment the tungsten target X-ray tube was excited to a peak voltage of 20.3 kv. corresponding to a maximum intensity wave length of 0.93 A. Thus, from Fig. 3, we find that within the uncertainty of the experiment the beam is better than 99% fluorescent K radiation.

If a significant amount of scattered radiation of short wave length is present in the fluorescent beam, the contrast difference in the pair of radiographs made on either side of the absorption edge will be diminished. Thus a beam diluted with scattered radiation will yield inaccurately low determinations of the critical element. Minimum dilution of the fluorescent beam with scattered incident radiation is essential for accurate quantitative measurements.

TABLE I
SAMPLE ORIGIN AND CROP YEAR

VARIETY	CLASS [b]	ORIGIN [a]	YEAR
Selkirk	HRS	Newell, S. D.; Fargo, N. D.; Williston, N. D.; Crookston, Minn.; Bozeman, Mont.	1963
Lee	HRS	Same as Selkirk	1963
Wichita	HRW	Manhattan, Hutchinson, Canton, Hays, Colby, and Garden City, Kansas	1960
Triumph	HRW	Lake Blackwell and Woodward, Okla.	1960
Omar	White	Pullman, Wash.	1963

[a] Kernels selected were from composite samples from the places indicated.
[b] HRS, hard red spring; HRW, hard red winter.

Specimens. The wheat kernel sections analyzed were taken from kernels selected from the samples listed in Table I.
The sections were obtained with a freezing stage microtome and were then placed in a controlled atmosphere at 71% r.h. to bring them to moisture equilibrium, in this case 14%. It is our experience that wheat kernels take about 3 weeks to reach moisture equilibrium in this controlled atmosphere. On this basis it was inferred that no detectable change in moisture content occurs while the section is out of the controlled atmosphere for a 100-min. X-ray exposure.

Results and Discussion

Quantitative Determination of Calcium Content. To map calcium concentrations within a section of endosperm, we note from Fig. 1 that the K absorption edge of calcium λ_{K-Ca} is at a wave length of 3.070 A and that this edge is bracketed by the characteristic Kα fluorescent radiation from a titanium target, λ_{Ti}, at 2.750 A, and the Kα fluorescent radiation from a calcium target, λ_{Ca}, at 3.360 A. A radiograph of the specimen is taken with each of these beams to the same background darkness. The Ti fluorescent beam will be absorbed more than the Ca fluorescent beam at points where calcium concentrations are located; the two radiographs record this as visible contrast differences. Weak contributions to the fluorescent beam from Kβ radiations are on the same side of the absorption edge as the Kα radiations, and thus serve to enhance the contrast.

Figures 4A and 4B are positive enlargements of a pair of such radiographs; white areas represent regions which have absorbed less of the beam. Note that there are few distinct white areas shown in Fig. 4A, which was taken with λ_{Ti} radiation for which the absorption

Fig. 4. Positive prints of radiographs obtained with fluorescent radiation: A (left), of wave length λ_{Ti} at 15 pkv., 20 ma. × 40 min.; B (center), of wave length λ_{Ca} at 12.5 pkv., 25 ma. × 135 min.; and C (right), a transmitted-light photomicrograph. The specimen is a section of Wichita hard red winter wheat 450 μ thick.


1.5 MM

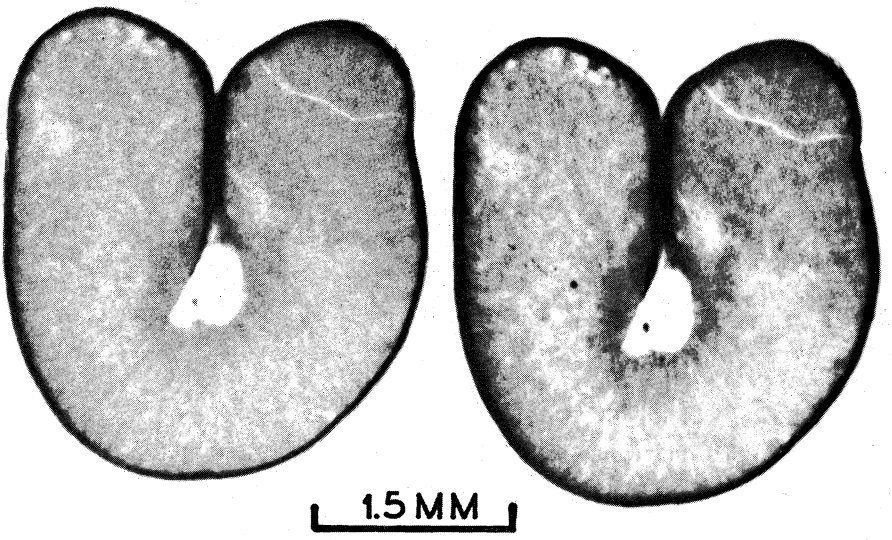
1.5 MM

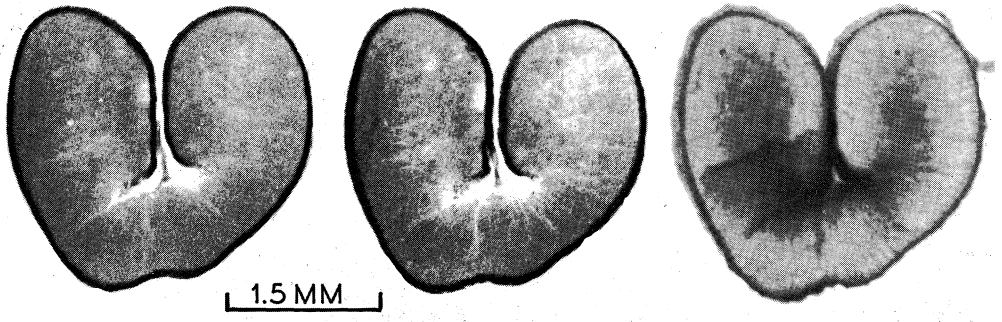
1.5 MM

coefficient of calcium is high. On the contrary, Fig. 4B, taken with λ_{Ca} radiation (for which the absorption coefficient of calcium is low) shows vivid white regions, corresponding to heavy penetration of the fluorescent beam. In this wheat kernel section there are regions in which λ_{Ti} radiation is heavily absorbed, but in which λ_{Ca} radiation is lightly absorbed; these regions are areas of high calcium concentration. In 4A and 4B, a radiograph of a section of a kernel of hard red winter wheat of the Wichita variety, the high calcium concentration is within the cell walls. This may be verified by comparing it with a transmitted-light photomicrograph, Fig. 4C, of the same specimen. White areas in both radiograph enlargements are low-density regions.

Figures 5 and 6 are additional enlargements of pairs of such radiographs. Figure 5, at A and B, shows a heavy calcium concentration within the outer and center regions (see Fig. 7) of the lower part of a section of Omar white wheat. Figure 6, A, B, and C, shows a slight calcium concentration within the cell walls of a section of Selkirk hard red spring wheat, and an outstanding calcium concentration in the center, cheek, and outer regions at the upper right.

Note that in Fig. 5 no cell-wall structure can be seen. The endosperm cells of Omar white wheat are much smaller than those of the other species investigated. To investigate the possibility of calcium concentration within the endosperm cell walls of this variety would require a much thinner section than those used, and a very fine-grain photographic emulsion. For that reason no photomicrograph is included in the figure.

The working equation for quantitative evaluation of calcium is derived in Appendix I as

$$m_1 = \frac{(\lambda_1/\lambda_2)^n \,\mathrm{Ln}\,\{(D_{02}-D_0)/(D_2-D_0)\} - \mathrm{Ln}\,\{(D_{01}-D_0)/(D_1-D_0)\}}{(\lambda_1/\lambda_2)^n\,\mu_{12}-\mu_{11}}$$

where m_1 is the mass per unit area of calcium; D_0 is the blackness of the X-ray film due to fog; D_{01} is the blackness of the film due to the incident X-ray beam of wave length λ_{Ti}, and D_{02} is the same quantity for λ_{Ca}; D_1 is the film blackness due to λ_{Ti} after passage through the sample, and D_2 is the same quantity for λ_{Ca}. The absorption coefficient

Fig. 5. Positive prints of radiographs obtained with fluorescent radiation: A (left), of wave length λ_{Ti} at 15 pkv., 20 ma. × 30 min.; B (right), of wave length λ_{Ca} at 12.5 pkv., 25 ma. × 100 min. The specimen is a section of Omar white wheat 315 μ thick.

Fig. 6. Positive prints of radiographs obtained with fluorescent radiation: A (left), of wave length λ_{Ti} at 15 pkv., 20 ma. × 30 min.; B (center), of wave length λ_{Ca} at 12.5 pkv., 25 ma. × 100 min.; and C (right), a transmitted-light photomicrograph. The specimen is a section of Selkirk hard red spring wheat 360 μ thick.

μ_{11} is for calcium irradiated with λ_{Ti}, and μ_{12} is for calcium irradiated with λ_{Ca}. In this wave length region the exponent n is 2.8.

Calcium is determined by measuring the blackness of appropriate regions of three developed films, one of which has been unexposed to determine the fog blackness, one of which has been exposed to fluorescent radiation of wave length λ_{Ti} in which part of the film has not been covered by the specimen, and the other has been similarly exposed to λ_{Ca}.

As a check of the quantitative technique, pieces of filter paper preboiled in distilled water were soaked in a solution of calcium nitrate in distilled water. The calcium content of the dried paper was determined by weighing and by area measurement. Two test samples were prepared, sample A having 1.25 γ/mm.^{2} and sample B having 6.26 γ/mm.^{2} of calcium. Radiographs of each artificially doped specimen were obtained with titanium, and calcium K radiation from fluorescent targets. Four sets of exposures of sample A and two sets of exposures of sample B were made. The results are presented in Table II. The calcium content obtained radiographically was well within 10% of the correct value, in the range of concentration investigated.

The sensitivity of the method is presently limited by the stability of the Photovolt 520-M photographic densitometer and Model 52 transmission density unit used to obtain these data. An error analysis (4, p. 65) has indicated that a variance in blackness measurement of 0.01 results in an error of 0.23 γ/mm.^{2} in the calcium determination, and a variance in blackness measurement of 0.001 yields an error of 0.02 γ/mm.^{2} In the present work the variance in blackness measurements was approximately 0.002 unit, corresponding to an average error in calcium determination of 0.05 γ/mm.^{2}

Results. The calcium concentration, in γ/mm.^{2}, in small areas of sections from seven different wheat kernels, appears in Table III.

TABLE II

RADIOGRAPHIC DETERMINATION OF CALCIUM CONTENT OF KNOWN SAMPLES

SAMPLE	NUMBER[a]	CALCIUM CONTENT		DEVIATION (MASSING — RADIOGRAPHY)	
		By Massing	By Radiography		
		γ/mm.^{2}	γ/mm.^{2}	γ/mm.^{2}	%
A	A1	1.25	1.31	−0.06	−4.8
A	A2	1.25	1.20	0.05	4.0
A	A3	1.25	1.28	−0.03	−2.4
A	A4	1.25	1.34	−0.09	−7.2
B	B1	6.26	6.86	−0.60	−9.6
B	B2	6.26	5.86	0.40	6.4

[a] A1 means the No. 1 pair of radiographs of paper sample A.

TABLE III
CALCIUM CONCENTRATION[a]

SAMPLE	OUTER		CHEEK		CENTER		CREASE		THICKNESS
	$\gamma/mm.$	%	$\gamma/mm.$	%	$\gamma/mm.$	%	$\gamma/mm.$	%	μ
Omar 1	0.9	0.22	n.d.[b]	0.00	0.8	0.18	0.3	0.08	317
Omar 2	0.4	0.08	n.m.[b]	n.m.	0.2	0.04	0.3	0.06	351
Selkirk 1	1.1	0.22	0.8	0.16	0.7	0.14	1.7	0.34	364
Selkirk 2	0.3	0.06	n.m.	n.m.	0.5	0.10	0.8	0.16	361
Lee	0.5	0.13	0.3	0.07	0.5	0.13	0.5	0.13	288
Wichita	2.5	0.40	0.5	0.08	0.7	0.11	1.4	0.23	452
Triumph	0.9	0.26	0.7	0.20	0.8	0.23	1.0	0.29	258

[a] Assigned density, 1.35 g./cm. at 14% moisture.
[b] n.d. = none detectable; n.m. = not measured.

Measurements were made in different endosperm regions (1) (outer, cheek, center, and crease) as shown in Fig. 7. The choice of the place at which the calcium content was measured in the same region of different kernels was determined by such factors as pitting of the sections, and the distribution of the calcium segregation.

The measurement in the outer region of the Wichita specimen is eight times as great as the average macroscopic calcium content of 0.05% obtained by other investigators (8). Most other measurements are two to three times the macroscopic averages. The larger values are not surprising, for we have measured specimens having no detectable calcium concentrations.

Percent calcium was computed with an assigned density of 1.35 g./cm.^{3}, at 14% moisture (9), which is consistent with the accuracy of this experiment.

Circular densitometer apertures of diameters 0.3 and 0.8 mm. were

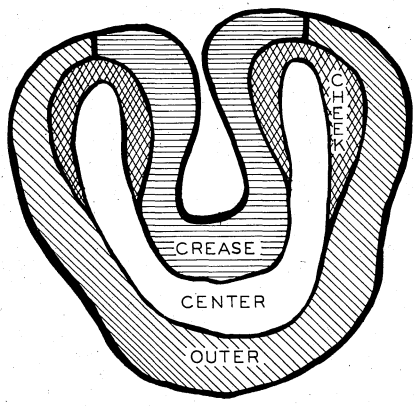

Fig. 7. Schematic drawing of a transverse section of a wheat kernel showing the four different endosperm regions.

used to obtain radiographic darkness. The Wichita and Triumph specimens listed in Table II were measured with the smaller aperture. Thus in the Triumph specimen calcium present in volumes of 0.018 mm.^{3} was determined. A sample this size that measured 0.2% calcium would contain 0.05 γ of calcium, a quantity at the lower limit of the capability of a microbalance.

Conclusion

The present investigation has demonstrated the feasibility of determining mineral content and its distribution in the endosperm in a quantitative way, through the application of microradiographic techniques, and by use of monochromatic radiography on either side of an absorption edge of the mineral element being studied. The calcium content of a wheat kernel section has been shown to increase from inside to bran of the kernel, in agreement with earlier workers who performed microchemical analysis of small samples removed with the aid of a dental drill. Because of the finer detail possible by the present technique, we have been able to find calcium concentration in cell walls. From this work we can infer clearly that calcium in a wheat kernel is quite nonuniform. We have found evidence of a range in calcium concentration of a factor of 5 in one kernel section of Wichita wheat, in which calcium concentration ranged from 0.08 to 0.40% in different parts of the kernel.

Acknowledgment

We thank A. Ward of the Flour and Feed Milling Department, Kansas State University, for supplying wheat samples, and E. J. Kobetich for assistance with machine computations.

Appendix I
Quantitative Measurements Using X-Rays

Definitions of the symbols used in the following text are as follows:

λ_i = The wave length of a monochromatic X-ray beam;
I_{0i} = Intensity of an X-ray beam of wave length λ_i before passage through the specimen;
I_i = Intensity of an X-ray beam of wave length λ_i after passage through the specimen;
D_{0i} = Radiographic blackness due to an X-ray beam of wave length λ_i before passage through the specimen;
D_i = Radiographic blackness due to an X-ray beam of wave length λ_i after passage through the specimen;
D_0 = Radiographic blackness of processed unexposed film, due to developer, etc.;
μ_i = Total X-ray mass absorption coefficient of the specimen at X-ray wave length λ_i;
a_j = The fractional mass of the specimen that is comprised of the element of the j^{th} kind;
m = Total mass per unit area of the specimen;

m_j = Mass per unit area of the j^{th} element in the specimen;
k_j = Proportionality constant for the j^{th} element which relates μ_{j1} to λ_1^n; and
μ_{j1} = X-ray mass absorption coefficient of element j at wave length λ_1.

Suppose a biological specimen is comprised of k elements and the mass per unit area of the j = 1 element is to be measured. The total X-ray mass absorption coefficient of a polyelemental specimen at an X-ray wave length λ_1 is given by

$$\mu_1 = a_1\mu_{11} + \sum_{j=2}^{k} a_j\mu_{j1}. \tag{1}$$

If no X-ray absorption edges of the elements j = 2,3,...k are bracketed by λ_1 and λ_2, then for the j^{th} element $\mu_{j1} = k_j\lambda_1^n$, and therefore

$$\mu_{j2} = (\lambda_2/\lambda_1)^n\mu_{j1}, \tag{2}$$

where n is a number close to 3.

Writing equation 1 for λ_2 and multiplying each term of the resulting equation by $(\lambda_1/\lambda_2)^n$ and then using equation 2, it is seen that

$$(\lambda_1/\lambda_2)^n\mu_2 = (\lambda_1/\lambda_2)^n a_1\mu_{12} + \sum_{j=2}^{k} a_j\mu_{j1}. \tag{3}$$

Writing equation 1 for λ_1 and subtracting the resulting equation from equation 3, the following equation is obtained:

$$(\lambda_1/\lambda_2)^n\mu_2 - \mu_1 = a_1[(\lambda_1/\lambda_2)^n\mu_{12} - \mu_{11}]. \tag{4}$$

Now for a monochromatic X-ray beam of wave length λ_1 passing through a polyelemental specimen

$$\mu_1 = (1/m)\,\mathrm{Ln}\,(I_{01}/I_1), \tag{5}$$

and for an X-ray beam of wave length λ_2

$$\mu_2 = (1/m)\,\mathrm{Ln}\,(I_{02}/I_2). \tag{6}$$

Making these substitutions for μ_1 and μ_2 into equation 4 and solving for $m_1(a_1\ m = m_1)$ yields

$$m_1 = \frac{(\lambda_1/\lambda_2)^n\,\mathrm{Ln}(I_{02}/I_2) - \mathrm{Ln}(I_{01}/I_1)}{(\lambda_1/\lambda_2)^n\mu_{12} - \mu_{11}}. \tag{7}$$

In Fig. 8 it is shown for film blackness of 0 to 2.0 that the product of (X-ray beam intensity) × (time), the X-ray exposure, is a linear function of the radiograph darkness for Kodak type-M X-ray film used in this investigation. This particular curve was obtained with fluorescent X-radiation from an iron target, though this is not of consequence to the argument and is included only as general information. Now since $D - D_0 = KI$, where K is a proportionality constant, equation 7 becomes

$$m_1 = \frac{(\lambda_1/\lambda_2)^n\,\mathrm{Ln}\,\{(D_{02} - D_0)/(D_2 - D_0)\} - \mathrm{Ln}\,\{(D_{01} - D_0)/(D_1 - D_0)\}}{(\lambda_1/\lambda_2)^n\mu_{12} - \mu_{11}}. \tag{8}$$

Equation 8 is the working equation for fluorescent X-ray quantitative analysis. The quantities labeled D are measured on the X-ray film with a densitometer, and λ_1 and μ_{1j} have been determined by others and are tabular, as for example, in the *Handbook of Chemistry and Physics*.

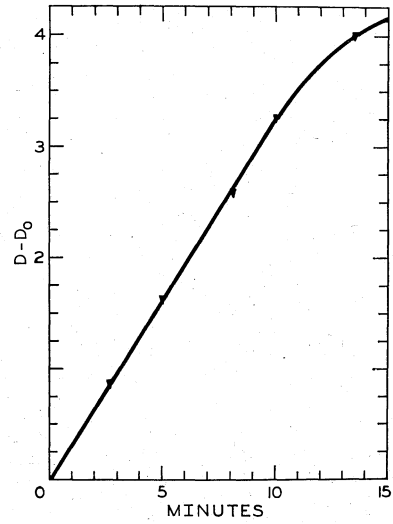

Fig. 8. Radiograph density *vs.* exposure time for Kodak Type M X-ray film. Over a considerable density range the quantity $(D - D_0)$ is directly proportional to the product of (X-ray intensity) × (time). Exposures were made with iron fluorescent radiation at an X-ray tube excitation of 18 pkv. and 20 ma.

Literature Cited

1. MORRIS, V. H., ALEXANDER, T. L., and PASCOE, E. D. Studies of the composition of the wheat kernel. I. Distribution of ash and protein in center sections. Cereal Chem. **22:** 351–360 (1945).
2. MORRIS, V. H., PASCOE, E. D., and ALEXANDER, T. L. Studies of the composition of the wheat kernel. II. Distribution of certain inorganic elements in center sections. Cereal Chem. **22:** 361–371 (1945).
3. SEMAT, HENRY. Introduction to atomic and nuclear physics (4th ed.). Holt, Rinehart, and Winston: New York (1962).
4. ENGSTROM, A. X-ray microanalysis in biology and medicine. Elsevier: New York (1962).
5. ROGERS, T. H. Production of monochromatic X-radiation for microradiography by excitation of fluorescent characteristic radiation. J. Appl. Phys. **23:** 881–887 (1952).
6. ROWLAND, R. E. Analysis of fluorescent X-radiation by means of proportional counters. J. Appl. Phys. **24:** 811–812 (1953).
7. SPLETTSTOSSER, H. R., and SEEMANN, H. E. Application of fluorescent X-rays to metallurgical microradiography. J. Appl. Phys. **23:** 1217–1222 (1952).
8. SCHRENK, W. G. Chemical composition of Kansas wheat. Tech. Bull. 79, Kansas State Univ., Manhattan, p. 14 (1955).
9. PETERS, W. R., and KATZ, R. Using a density gradient column to determine wheat density. Cereal Chem. **39:** 487–494 (1962).